

Naphthoxaphospholes as examples of fluorescent *phospha-acenes*†Feng Li Laughlin,^a Arnold L. Rheingold,^b Nihal Deligonul,^a Brynna J. Laughlin,^c Rhett C. Smith,^c Lee J. Higham^d and John D. Protasiewicz^{*a}

Received 25th April 2012, Accepted 6th July 2012

DOI: 10.1039/c2dt30902e

Seven new fluorescent 2-R-naphtho[2,3-*d*]oxaphospholes (R-NOPs) (**4a–g**; R = ^tBu (**a**), Ad (**b**), C₆H₅ (**c**), 4-MeC₆H₄ (**d**), 4-ClC₆H₄ (**e**), 4-BrC₆H₄ (**f**), 4-MeOC₆H₄ (**g**)), have been synthesized by cyclocondensation reactions of benzimidoyl chlorides with 3-phosphino-2-naphthol (**3**). The compounds were characterized by multinuclear NMR, UV-vis, and fluorescence spectroscopy. Compounds **4a–d** and **4g** were characterized by cyclic voltammetry experiments. The solid state structures of compounds **4b** and **4d** were also determined by single-crystal X-ray diffraction experiments.

Introduction

2-Substituted 1,3-benzoxaphospholes (R-BOPs, Chart 1), first reported by Heinicke *et al.*,^{1–3} are fascinating conjugated heterocyclic molecules featuring phosphorus–carbon double bonds.⁴ In particular, they are unusual in that unlike phosphalkenes (RP=CR₂), they display significant fluorescence and are quite thermally stable despite lacking sterically demanding groups that are often required to afford kinetic stability to many phosphalkenes.^{5–9}

We have recently expanded on the synthesis of R-BOPs, and pioneered the synthesis of the difunctional analogues 2,6-disubstituted-benzo[1,2-*d*:4,5-*d'*]bisoxaphospholes (R₂-BBOPs, Chart 1).¹⁰ These conjugated materials were determined to have quantum yields reaching as high as 0.63. In addition, detailed

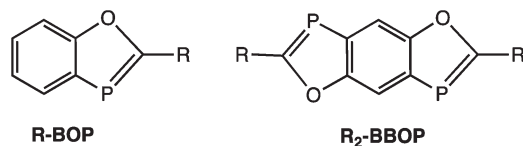


Chart 1 Structures of previously studied benzoxaphospholes.

^aDepartment of Chemistry, Case Western Reserve University, Cleveland, Ohio, 44106, USA. E-mail: protasiewicz@case.edu

^bDepartment of Chemistry and Biochemistry, University of California, San Diego, La Jolla, California 92093, USA.

E-mail: arheingold@ucsd.edu

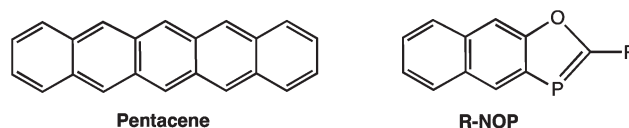
^cDepartment of Chemistry and Center for Optical Materials Science and Engineering Technologies (COMSET), Clemson University, Clemson, South Carolina 29634, USA

^dSchool of Chemistry, Newcastle University, Newcastle upon Tyne, NE1 7RU, UK. E-mail: lee.higham@ncl.ac.uk

†Electronic supplementary information (ESI) available: Details of synthesis for **1** and **2**, crystallographic, electrochemical, UV-vis, fluorescence, and computational details. CCDC 878276–878278. For ESI and crystallographic data in CIF or other electronic format see DOI: 10.1039/c2dt30902e

examination of the electrochemistry of these compounds confirmed that like phosphalkenes, these materials also feature lower lying LUMO orbitals introduced by the presence of the P=C functionality. This aspect of phosphalkene chemistry makes such compounds more electron deficient compared to molecules where a C=C bond exists in place of a P=C unit.¹¹ Many multiply bonded organophosphorus compounds having P=C units behave in a chemical manner similar to C=C containing molecules, hence, such compounds have often been called “carbon copies”.⁵ Yet the increased facility that phosphalkenes can undergo reduction offers new possibilities for applications.

Pentacenes (and related acenes) are a well studied class of molecules having much promise for use as molecular organic semi-conductors and field effect transistors.¹² Pentacene (Chart 2, left) is a purple material that slowly degrades in air and light. Much effort has gone into the design and synthesis of new acenes that can be accessed in high purity and that also possess increased stability, solubility, and appropriate solid state morphologies. The air stability of such materials could be enhanced if the overall potentials of the materials are lowered. *N*-Heteroacenes have been investigated for this purpose.¹³ A lot of recent work has appeared on the development of conjugated materials built around phospholes as integrated units in phosphorus-containing heteroacenes.^{14,15} In this report we detail the synthesis and full characterization of expanded versions of R-BOPs, 2-R-naphtho[2,3-*d*]oxaphospholes (R-NOPs, Chart 2, right). This study represents the first step towards creation of a series of increasingly extended electron deficient acene-like planar materials featuring bona-fide P=C bonds.

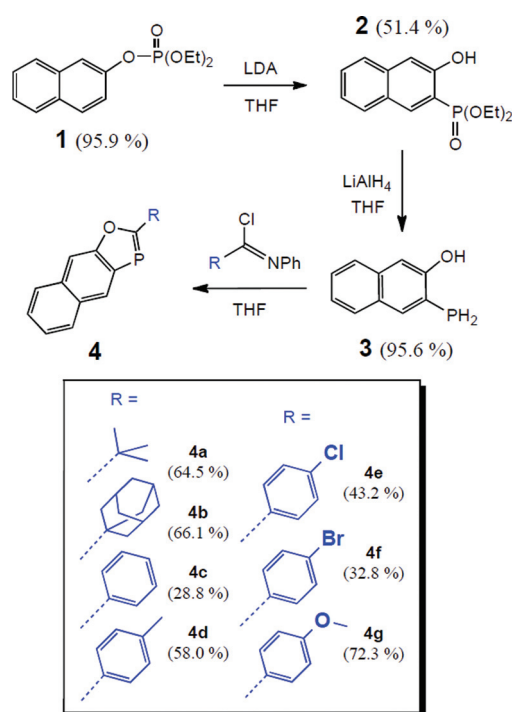
Chart 2 Comparison between pentacene and a *phospha-acene*.

Results and discussion

1. Syntheses and NMR properties

The route to R-NOPs required the synthesis of the previously unknown 3-phosphino-2-naphthol (**3**). Following the procedures developed by Dhawan and Redmore,¹⁶ the immediate precursor to this material, diethyl(3-hydroxy-2-naphthyl) phosphonate (**2**) could be accessed by application of an anionic *phospho*-Fries rearrangement of readily available diethyl(2-naphthyl)phosphate (**1**) (Scheme 1).

Single crystals of **2** suitable for an X-ray diffraction study were obtained from hexanes at $-45\text{ }^{\circ}\text{C}$. The internal metrics for **2** are unexceptional, but the presence of intermolecular $\text{P}=\text{O}\cdots\text{HO}$ hydrogen bonding leads to chains of molecules along the *c*-axis (Fig. 1).



Scheme 1 Synthesis of R-NOPs.

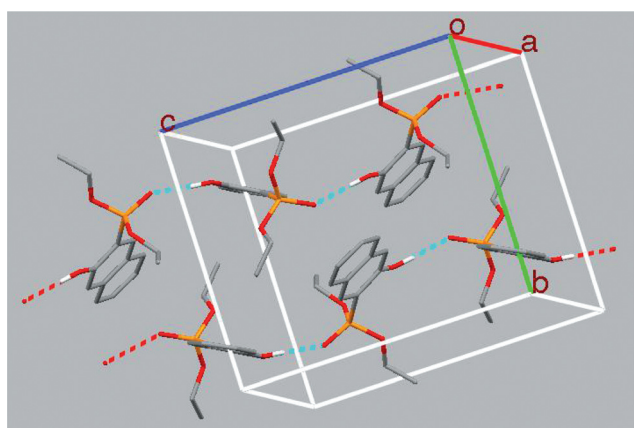


Fig. 1 Packing diagram of **2** showing intermolecular hydrogen bonding.

Compound **2** was thus reduced using LiAlH_4 to form compound **3** in 95.6% yield. Interestingly, this white solid displays much greater air stability than typical primary phosphines. For example, solutions of **3** in CDCl_3 solution at room temperature persist for a month or more without signs of decomposition (as ascertained by ^1H and $^{31}\text{P}\{^1\text{H}\}$ NMR spectroscopy). In the solid state compound **3** is stable for several months or longer.

Compound **3** thus possesses greater air-stability than the 2-phosphino-naphthalene, which decomposes slowly in CDCl_3 (72% of 2-phosphino-naphthalene remains after 7 days¹⁷). An interesting predictive model for the enhanced stability of select primary phosphines has recently been forwarded by Higham and coworkers.^{17,18} Two electronic factors were found to be important. First, primary phosphines possessing extended conjugation and/or heteroatoms were found to have HOMOs that were dislocated from the phosphino functionality and enhanced air-stability. Second, the products of oxidation of the primary phosphines, radical cations, having SOMO energy levels above -10 eV will have enhanced air-stability. The oxidized phosphines $[\text{RPH}_2]^+$, are postulated to be involved in the air oxidation of phosphines. We have thus undertaken analogous DFT calculations on $\mathbf{3}^{\cdot+}$. DFT studies on the radical cation of 2-phosphino-naphthalene reveals a SOMO energy level of -10.64 eV , while similar calculations on the $\mathbf{3}^{\cdot+}$ show a SOMO energy level of -10.72 eV (see ESI†). One might initially predict less air-stability for compound **3** compared to 2-phosphino-naphthalene, but as Fig. 2 reveals, the SOMO of $\mathbf{3}^{\cdot+}$ has no significant phosphorus contributions. The special enhanced stability of **3** might thus be particularly attributed to a shift in the SOMO away from phosphorus (unlike 2-phosphino-naphthalene). An interesting alternative explanation might lie in the nature of the hydroxy substituent, for it has been shown that oxidation of secondary phosphines can be inhibited by hydroquinones.¹⁹

The synthesis of R-NOPs **4a–g** was effected by the cyclocondensation of benzimidoyl chlorides with **3** in THF under

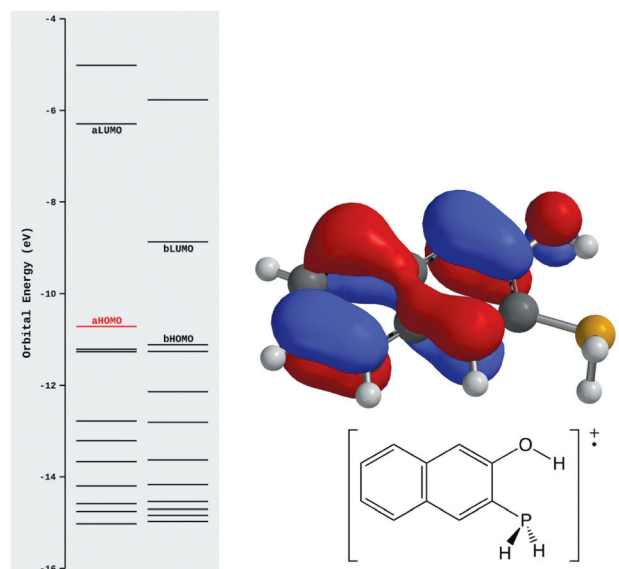


Fig. 2 MO diagram and SOMO for radical cation of **3**.

nitrogen. Yields ranged from modest to good, owing to the difficulty in purifying the products from similarly soluble starting materials and the anilinium salts. Compounds **4a–g** were isolated as crystalline white (**4a,b**) or yellow (**4c–g**) solids that possessed reasonable air and water stability, especially in the solid state. The R-NOPs were readily identified by characteristic $^{31}\text{P}\{^1\text{H}\}$ NMR chemical shifts resonating between 72.8–86.6 ppm, consistently *ca.* 2–3 ppm upfield from similarly substituted R-BOPs.¹⁰ Likewise, $^{13}\text{C}\{^1\text{H}\}$ NMR chemical shifts for the P=C carbons were consistently located 2.8–3.6 ppm upfield (between 198.3 to 217.9 ppm) for R-NOP *versus* R-BOP pairs. The $^1J_{\text{P}=\text{C}}$ coupling constants are *ca.* 63 Hz for alkyl substituted R-NOPs, and *ca.* 55 Hz for aryl substituted R-NOPs.

2. Structural studies of NOPs

Single crystals of **4b** and **4d** were subjected to X-ray diffraction analyses, and the results are shown in Fig. 3 and 4 in the form of ORTEP structural diagrams. For compound **4d**, the crystal contains two crystallographic independent molecules of **4d**.

Within the NOP rings, the atoms are co-planar. The P=C bond lengths for **4b** and **4d** are 1.700(3) and 1.716(3)/1.723(2) Å, respectively, and are consistent with the presence of a phosphorus–carbon double bond. Compound **4d** has a slightly longer bond length, possibly attributable to the extended conjugation of the NOP ring with the attached phenyl group. Notably, this ring lies in the plane of the NOP system with a maximum twist from

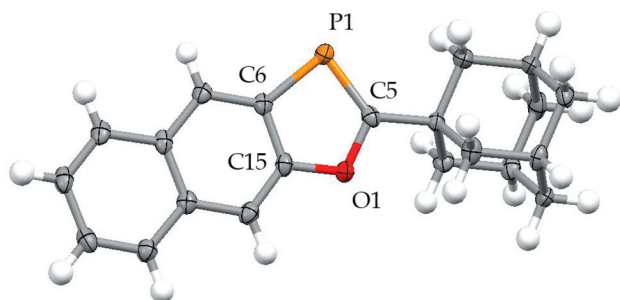


Fig. 3 ORTEP diagram of **4b**. Selected bond lengths (Å) and angles (°): P(1)–C(5), 1.700(3); P(1)–C(6), 1.806(3); O(1)–C(15), 1.373(3); O(1)–C(5), 1.386(3); C(5)–P(1)–C(6), 88.3(1); C(15)–O(1)–C(5), 110.6(2); O(1)–C(5)–P(1), 116.9(2).

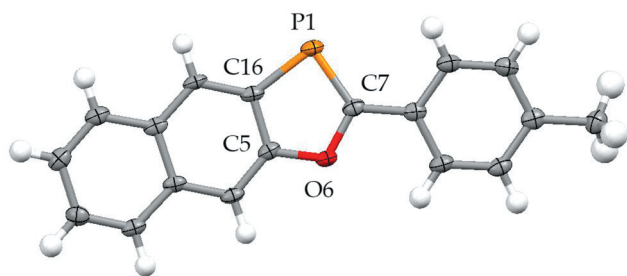


Fig. 4 ORTEP diagram of one of two independent molecules of **4d**. Selected bond lengths (Å) and angles (°): P(1)–C(7), 1.716(3); P(1)–C(16), 1.789(3); O(6)–C(5), 1.373(3); O(6)–C(7), 1.374(3); C(7)–P(1)–C(16), 88.0(1); C(5)–O(6)–C(7), 110.9(2); O(6)–C(7)–P(1), 116.6(2).

coplanarity of 7.6°. The angles about the phosphorus atoms in **4b** and **4d** are very similar (88.0–88.3°). For pentacenes, the crystal packing is an important consideration for their use. The crystal packing of **4b** is unexceptional, but the packing of molecules of **4d** is more interesting in the crystal lattice as displayed in Fig. 5. The packing may be described as herringbone-like with aromatic CH groups directed towards the aromatic systems of other molecules (closest CH...C distance is 2.78 Å).

3. Absorption and emission spectroscopy of NOPs

The UV-vis absorption spectra of **4a–g** are shown in Fig. 6 and 7. The data reveal π – π^* transitions for the alkyl-NOP derivatives **4a** and **4b** both at 333 nm (Fig. 6). Aryl-NOPs (**4c–g**), by contrast, show π – π^* transitions varying from 353 to 360 nm (Fig. 7). Similar bathochromic shifts (\sim 30 nm) are also observed between alkyl and aryl substituted BOPs.¹⁰ These trends are also reproduced by DFT calculations (*vide infra*). Over the concentration range 10^{-6} to 10^{-5} M the absorption data showed no evidence for aggregation for **4a–g**.

Compounds **4a–g** are notably fluorescent under UV light, appearing violet to blue in color. As for the absorption spectra, the fluorescence behavior for these compounds break down into

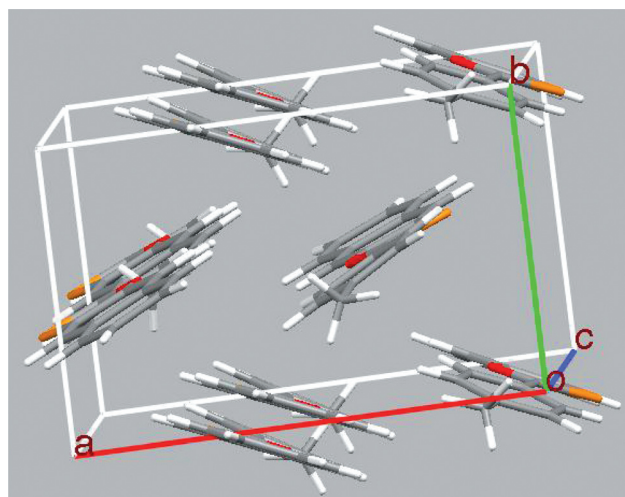


Fig. 5 Packing diagram for compound **4d**.

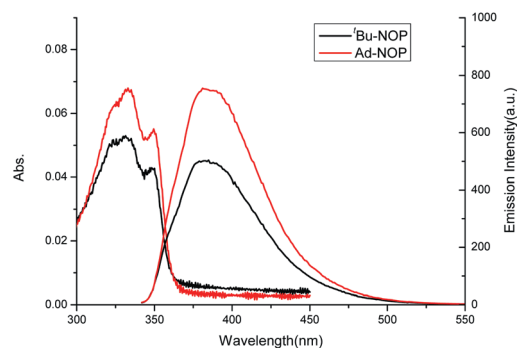


Fig. 6 UV-vis and fluorescence spectra for **4a** and **4b** in CH_2Cl_2 .

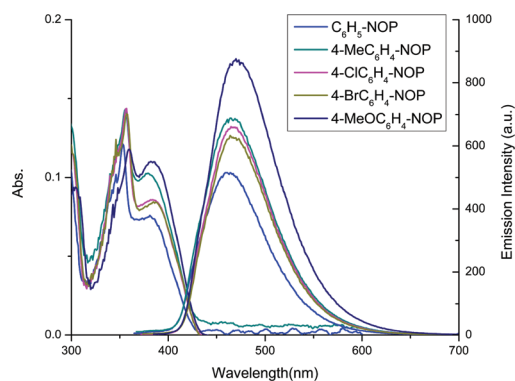


Fig. 7 UV-vis and fluorescence spectra for **4c–g** in CH_2Cl_2 .

Table 1 UV-vis and fluorescence spectra for **4a–g** in CH_2Cl_2

R	λ_{max} (nm)	$\lambda_{\text{F,max}}$ (nm)	Φ_{F}	τ (ns)	
4a	^t Bu	333	385	0.23	1.24(2)
4b	Ad	333	381	0.26	1.26(1)
4c	C_6H_5	353	461	0.12	0.76(1)
4d	4-Me C_6H_4	356	464	0.14	0.75(1)
4e	4-Cl C_6H_4	357	465	0.13	0.44(1)
4f	4-Br C_6H_4	357	464	0.13	0.80(5)
4g	4-MeOC $_6\text{H}_4$	360	470	0.22	0.84(1)

two sets of behavior based on the identity of the R substituents. The aryl substituted compounds **4c–g** displayed λ_{em} maxima from 461–470 nm, while the alkyl substituted derivatives **4a** and **4b** showed maxima around 383 nm (Table 1). Compared to comparably substituted R-BOPs,¹⁰ R-NOPs exhibited about a 40 nm wavelength redshift for λ_{em} maxima.

While there are significant parallels in the absorption and fluorescence spectra of R-BOPs and R-NOPs, there are striking differences in the measured quantum yields (Φ_{F}). In a series of BOPs, aryl substituted BOPs showed quantum yields (0.56–0.69 for Φ_{F}) that were over ten times greater than alkyl-substituted analogues.¹⁰ By contrast, all of the R-NOPs not only have significant fluorescence, but it is the alkyl substituted R-NOPs that have the greater quantum yields. Specifically, compounds **4a** and **4b** have quantum yields of 0.23 and 0.26, respectively, while compounds **4c–f** have Φ_{F} in the range of 0.12–0.14, except **4g** which shows Φ_{F} of 0.22. The reasons for these observations are not clear at this time.

4. Electrochemical and computational studies of NOPs

Electrochemical experiments were performed on several representative R-NOPs to probe their facility towards reduction in THF. Cyclic voltammograms of compounds **4a–d** and **4g** are thus shown in Fig. 8.

Two types of electrochemical behavior were displayed for the NOPs. The alkyl-NOPs **4a** and **4b** did not show evidence for reduction within the electrochemical window examined. By contrast, aryl substituted R-NOPs **4c**, **4d** and **4g** show quasi-reversible reduction waves ($i_{\text{pa}}/i_{\text{pc}} \sim 0.6$) between -1.8 to -1.9 V vs. SCE (see Table 2).

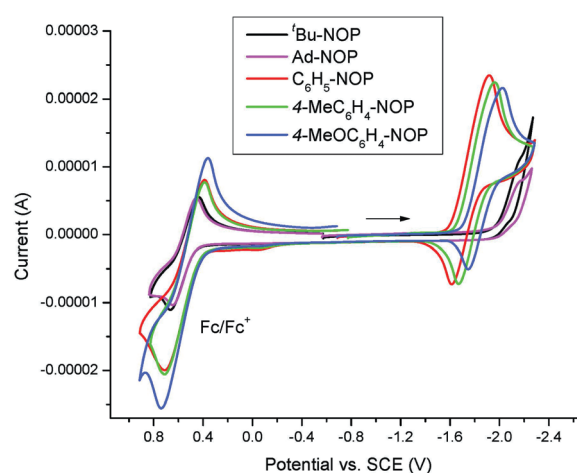


Fig. 8 Cyclic voltammograms for compounds **4a–d** and **4g**, in THF with 0.1 M [^tBu₄N][BF₄].

Table 2 Cyclic voltammograms for compounds **4a–d** and **4g**, in THF with 0.1 M [^tBu₄N][BF₄]

	E_{pc}	E_{pa}	$E_{(\text{pc} + \text{pa})/2}$
4a	—	—	—
4b	—	—	—
4c	−1.92	−1.61	−1.77
4d	−1.96	−1.67	−1.82
4g	−2.02	−1.75	−1.89

As one might expect, as the electron donating ability of the $p\text{-XC}_6\text{H}_4$ moves from H to Me and OMe, the reduction becomes more difficult. Overall, the R-NOPs (R = aryl) reduction occurs more readily than analogous R-BOPs (by 13–14 mV).¹⁰

Many of the above experimental trends observed between sets of electrochemical data of R-NOPs and R-BOPs can be reproduced by DFT calculations. Fig. 9 shows a comparison of the frontier molecular orbitals of Ph-NOP and Ph-BOP. The nature of the HOMOs and LUMOs are very similar between the pair of compounds. The greatest difference lies in the smaller HOMO–LUMO gap for Ph-NOP (3.39 eV vs. 3.84 eV).

A similar comparison can be made for Ph-NOP and ^tBu-NOP, in order to illustrate differences between alkyl and aryl substituted NOP compounds. Fig. 10 shows that the *tert*-butyl derivative has HOMO and LUMO orbitals that are localized only on the NOP ring system, and has a greater HOMO–LUMO gap (3.97 vs. 3.39 eV). The 0.52 eV higher lying LUMO orbital correlates with the inability to observe the reduction of the alkyl-substituted NOP derivatives.

Conclusions

The synthesis and detailed characterization of a new class of fluorescent compounds having low coordinate multiply bonded phosphorus atoms have been presented. The data support the conclusion that these materials possess greater conjugation than previously reported R-BOP species. The synthesis of the

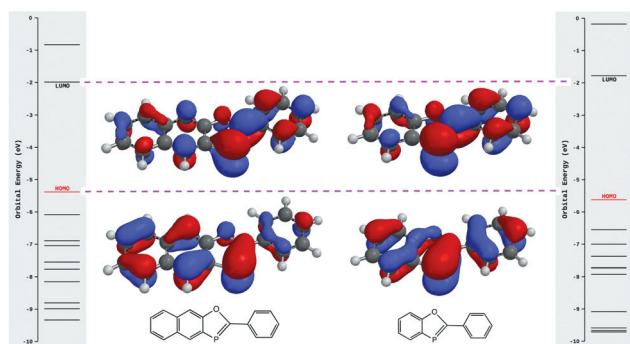


Fig. 9 MO diagrams for Ph-NOP and Ph-BOP.

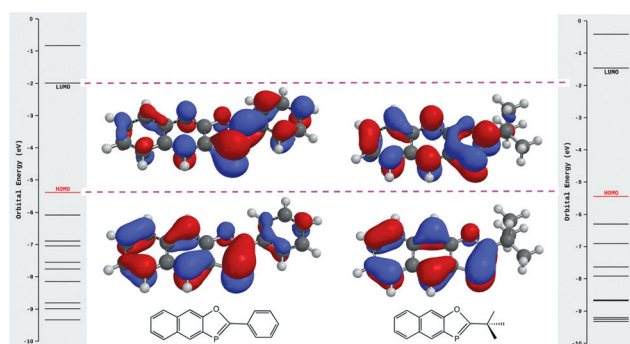


Fig. 10 MO diagrams for Ph-NOP and *t*-Bu-NOP.

difunctional analogues of NOPs is now underway to strive towards new conjugated low band gap analogues of pentacenes featuring phosphorus atoms participating in conjugation with the aromatic system.

Experimental

General considerations

Reactions were conducted under nitrogen using either Schlenk line techniques or within an MBraun drybox. Tetrahydrofuran, toluene and diethyl ether were dried by distillation from sodium and benzophenone ketyl. Hexanes was dried by distillation from sodium and benzophenone in the presence of tetraethylene glycol dimethyl ether. Methylene chloride was dried by distillation from calcium hydride. Methylene chloride (99.8%, for spectroscopy) and ethanol (200 proof) were degassed prior to use for UV-vis and fluorescence measurements. Benzimidoyl chlorides were prepared following literature protocols. NMR spectra (^1H and $^{31}\text{P}\{^1\text{H}\}$) were recorded in CDCl_3 on a Varian INOVA AS-400 spectrometer operating at 399.7 and 161.8 Hz, respectively, and $^{31}\text{P}\{^1\text{H}\}$ NMR were referenced to 85% H_3PO_4 . $^{13}\text{C}\{^1\text{H}\}$ NMR spectra were recorded in CDCl_3 on a Varian INOVA AS-600 spectrometer operating at 150.9 Hz. UV-vis and fluorescence spectra were recorded using a Cary-5G-UV-vis-NIR spectrophotometer and a Cary Eclipse spectrometer, respectively. Anthracene in ethanol was used as a standard for quantum yield measurements (conc. 5.0×10^{-6} M). Lifetime measurements

were made using an EasyLife II lifetime fluorimeter from Photon Technology International, Inc. The excitation slit width for all measurements was kept at default settings (5 nm). Melting points were measured on a Thomas Hoover Capillary Melting Point Apparatus. Elemental analyses were performed by Robertson Microлит Laboratories, Ledgewood, New Jersey. High resolution mass spectrometry was performed by the University of Michigan Mass Spectrometry facility using a VG (Micromass) 70-250-S magnetic sector spectrometer with EI technique at 70 eV.

3-Phosphino-2-naphthol (**3**)

Diethyl (3-hydroxy-2-naphthyl)phosphonate (**2**, 4.02 g, 14.3 mmol) was added to a 500 mL round bottom flask containing a solution of LiAlH_4 (1.09 g, 28.6 mmol) in 100 mL of THF and a stir bar. The solution was stirred and refluxed under nitrogen for 1 hour. The flask was opened and an aqueous solution of saturated ammonium chloride was added drop wise to quench the excess LiAlH_4 . The mixture was extracted with chloroform (200 mL) and the organic layer was separated and then filtered through celite using a glass fritted filter funnel. The filtrate was evaporated by rotary evaporation to yield white solid **3** (2.41 g, 95.6%). ^1H NMR (CDCl_3): δ 8.04 (d, 1H, $^3J_{\text{PH}} = 9.6$ Hz), 7.72 (m, 1H), 7.66 (m, 1H), 7.43 (m, 1H), 7.33 (m, 1H), 7.17 (d, 1H, $^4J_{\text{PH}} = 2.4$ Hz), 5.29 (s, 1H, OH), 4.20 (s, 1H, PH), 3.69 (s, 1H, PH); $^{31}\text{P}\{^1\text{H}\}$ NMR (CDCl_3): δ -148.3 (s). $^{13}\text{C}\{^1\text{H}\}$ NMR (CDCl_3): δ 154.4 (d, $J_{\text{PC}} = 4.7$ Hz), 137.4 (d, $J_{\text{PC}} = 22.3$ Hz), 135.4, 128.9 (d, $J_{\text{PC}} = 8.0$ Hz), 127.3, 127.0, 126.1, 123.9, 117.3 (d, $J_{\text{PC}} = 12.2$ Hz), 109.0 (d, $J_{\text{PC}} = 1.4$ Hz); mp: 134–135 °C; Elemental Analysis: Calc. for $\text{C}_{10}\text{H}_9\text{OP}$ (M.W. 176.15), C 68.18%, H 5.15%; found: C 67.91%, H 5.10%.

2-(*tert*-Butyl)naphtho[2,3-*d*]oxaphosphole (**4a**)

3-Phosphino-2-naphthol (**3**, 1.00 g, 5.68 mmol) and *N*-phenylpivalimidoyl chloride (3.67 g, 18.8 mmol) were added to a 250 mL round bottom flask with a stir bar, and the flask was outfitted with a reflux condenser and then flushed with nitrogen. THF (35 mL) was added by cannula to the flask and the solution was refluxed for 15 hours. The reaction mixture was taken into a dry box, and filtered using glass fritted filter funnel. The solid was extracted 2 times with THF (~5 mL) and the combined filtrate was evaporated under vacuum yield a brown solid. Purification by column chromatography (CH_2Cl_2 –hexanes 1 : 9, $R_f = 0.8$) led to isolation of white solid **4a** (0.89 g, 65%). ^1H NMR: δ 8.40 (d, 1H, $^3J_{\text{PH}} = 4.0$ Hz), 8.08 (s, 1H), 7.93 (m, 2H), 7.47 (m, 2H), 1.52 (d, 9H, $^4J_{\text{HH}} = 1.2$ Hz); $^{31}\text{P}\{^1\text{H}\}$ NMR: δ 74.1 (s); $^{13}\text{C}\{^1\text{H}\}$ NMR: δ 217.6 (d, $J_{\text{PC}} = 63.6$ Hz), 158.6, 136.2 (d, $J_{\text{PC}} = 38.1$ Hz), 132.4 (d, $J_{\text{PC}} = 2.3$ Hz), 129.9 (d, $J_{\text{PC}} = 9.2$ Hz), 128.4 (d, $J_{\text{PC}} = 19.2$ Hz), 127.7, 127.6, 125.8, 124.4, 108.8, 38.4 (d, $J_{\text{PC}} = 11.8$ Hz), 29.7 (d, $J_{\text{PC}} = 9.1$ Hz); UV (CH_2Cl_2): λ_{max} , nm (ϵ , $\text{M}^{-1} \text{cm}^{-1}$) 333 (12398); Fluorescence (CH_2Cl_2 , 5×10^{-6} M): λ_{ex} , nm (Int.) 385 (504); Quantum yield (CH_2Cl_2): Φ_{F} 0.229; mp: 77–80 °C; Elemental analysis: Calc. for $\text{C}_{15}\text{H}_{15}\text{OP}$ (M. W. 242.25), C 74.37%, H 6.24%; found: C 73.80%, H 6.20%.

2-(Adamantyl)naphtho[2,3-*d*]oxaphosphole (4b)

3-Phosphino-2-naphthol (**3**, 0.600 g, 3.41 mmol) and *N*-adamantyl-phenylbenzimidoyl chloride (1.73 g, 6.32 mmol) were added in a 250 mL round bottom flask with a stir bar, and the flask was outfitted with a reflux condenser and then flushed with nitrogen. THF (25 mL) was added to the flask by cannula under nitrogen. The solution was refluxed for 15 hours. The reaction mixture was taken into a dry box, and filtered using glass fritted filter funnel. The solid was extracted 2 times with THF (~5 mL) and the combined filtrate was evaporated under vacuum yield a brown solid. Purification by column chromatography (CH₂Cl₂–hexanes 1 : 9, *R_f* = 0.8) led to white solid **4b** (0.72 g, 66%). ¹H NMR: δ 8.44 (d, 1H, ³*J*_{PH} = 4.0 Hz), 8.07 (s, 1H), 7.93 (m, 2H), 7.46 (m, 2H), 2.13 (s, 9H), 1.83 (s, 6H); ³¹P{¹H} NMR: δ 72.8 (s); ¹³C{¹H} NMR: δ 217.9 (d, *J*_{PC} = 62.8 Hz), 158.4, 136.1 (d, *J*_{PC} = 38.1 Hz), 132.3 (d, *J*_{PC} = 2.1 Hz), 129.8 (d, *J*_{PC} = 9.4 Hz), 128.4 (d, *J*_{PC} = 19.2 Hz), 127.7, 127.6, 125.7, 124.3, 108.7, 41.8 (d, *J*_{PC} = 9.4 Hz), 40.3 (d, *J*_{PC} = 10.9 Hz), 36.7, 28.3 (d, *J*_{PC} = 1.4 Hz); UV (CH₂Cl₂): λ_{max}, nm (ε, M⁻¹ cm⁻¹) 333 (10972); Fluorescence (CH₂Cl₂, 5 × 10⁻⁶ M): λ_{ex}, nm (Int.) 381 (755); Quantum yield (CH₂Cl₂): Φ_F 0.256; mp: 145–147 °C; Elemental analysis: Calc. for C₂₁H₂₁OP (M. W. 320.36), C 78.73%, H 6.61%; found: C 78.52%, H 6.82%.

2-(Phenyl)naphtho[2,3-*d*]oxaphosphole (4c)

3-Phosphino-2-naphthol (**3**, 0.350 g, 1.99 mmol) and 4-methoxy-*N*-phenylbenzimidoyl chloride (1.28 g, 5.93 mmol) were added in a 250 mL round bottom flask with a stir bar, and the flask was outfitted with a reflux condenser and then flushed with nitrogen. THF (25 mL) was added to the flask by cannula under nitrogen. The solution was refluxed for 20 hours. The reaction mixture was taken into a dry box and filtered using glass fritted filter funnel. The solid on the frit was extracted 2 times with THF (~5 mL) and the combined filtrate was evaporated under vacuum yield a brown solid. This solid was dissolved in CH₂Cl₂ (~75 mL), and the solution was washed successively with degassed solutions of aqueous HCl (1.2 M, 100 mL), aqueous NaOH (1 M, 100 mL) and distilled H₂O (100 mL). The solvent was removed under vacuum to yield a yellow solid, which was washed with degassed ethanol (~150 mL) and then recrystallized from toluene at –45 °C to yield yellow solid **4c** (0.150 g, 28.8%). ¹H NMR: δ 8.51 (d, 1H, ³*J*_{PH} = 3.2 Hz), 8.17 (s, 1H), 8.11 (m, 2H), 7.96 (m, 2H), 7.47 (m, 5H); ³¹P{¹H} NMR: δ 83.7 (s); ¹³C{¹H} NMR: δ 199.9 (d, *J*_{PC} = 55.3 Hz), 158.0, 136.6 (d, *J*_{PC} = 37.3 Hz), 134.6 (d, *J*_{PC} = 12.8 Hz), 132.9 (d, *J*_{PC} = 2.9 Hz), 130.3 (d, *J*_{PC} = 5.0 Hz), 130.1 (d, *J*_{PC} = 10.3 Hz), 128.9, 128.7, 127.8, 127.7, 126.1, 125.1 (d, *J*_{PC} = 14.8 Hz), 124.7, 109.1; UV (CH₂Cl₂): λ_{max}, nm (ε, M⁻¹ cm⁻¹) 353 (24246); Fluorescence (CH₂Cl₂, 5 × 10⁻⁶ M): λ_{ex}, nm (Int.) 461 (516); Quantum yield (CH₂Cl₂): Φ_F 0.121; mp: 173–176 °C; Elemental analysis: Calc. for C₁₇H₁₁OP (262.24), C 77.86%, H 4.23%; found: C 77.63%, H 4.16%.

2-(4-Methylphenyl)naphtho[2,3-*d*]oxaphosphole (4d)

3-Phosphino-2-naphthol (**3**, 1.00 g, 5.68 mmol) and 4-methyl-*N*-phenylbenzimidoyl chloride (1.95 g, 8.52 mmol) were added in

a 250 mL round bottom flask with a stir bar. The flask was outfitted with a reflux condenser and flushed with nitrogen and THF (30 mL) was added by cannula. The solution was refluxed for 20 hours. The reaction mixture was taken into a dry box and filtered using glass fritted filter funnel. The solid on the frit was extracted 2 times with THF (~5 mL) and the combined filtrate was evaporated under vacuum yield a brown solid. The solid was dissolved in CH₂Cl₂ (~75 mL), washed successively with degassed solutions of aqueous HCl (1.2 M, 100 mL), aqueous NaOH (1 M, 100 mL) and distilled H₂O (100 mL). The solvent was removed under vacuum to yield a yellow solid which was washed with degassed ethanol (~150 mL) and recrystallized from toluene at –45 °C to yield yellow solid **4d** (0.910 g, 58.0%). ¹H NMR: δ 8.47 (d, 1H, ³*J*_{PH} = 2.8 Hz), 8.13 (s, 1H), 7.98 (m, 2H), 7.93 (m, 2H), 7.47 (m, 2H), 7.25 (d, 2H, ³*J*_{HH} = 5.2 Hz), 2.41 (s, 3H); ³¹P{¹H} NMR: δ 80.1 (s); ¹³C{¹H} NMR: δ 200.3 (d, *J*_{PC} = 55.6 Hz), 158.0 (d, *J*_{PC} = 3.5 Hz), 140.7 (d, *J*_{PC} = 5.0 Hz), 136.8 (d, *J*_{PC} = 37.1 Hz), 132.8 (d, *J*_{PC} = 2.6 Hz), 132.0 (d, *J*_{PC} = 13.0 Hz), 130.1 (d, *J*_{PC} = 10.3 Hz), 129.6, 128.6 (d, *J*_{PC} = 19.2 Hz), 127.7, 127.7, 126.0, 125.1 (d, *J*_{PC} = 14.6 Hz), 124.6, 109.0, 21.6; UV (CH₂Cl₂): λ_{max}, nm (ε, M⁻¹ cm⁻¹) 356 (28654); Fluorescence (CH₂Cl₂, 5 × 10⁻⁶ M): λ_{ex}, nm (Int.) 464 (689); Quantum yield (CH₂Cl₂): Φ_F 0.140; mp 170–174 °C; Elemental analyses: Calc. for C₁₈H₁₃OP (M. W. 276.27), C 78.25%, H 4.74%; found: C 78.36%, H 4.96%.

2-(4-Chlorophenyl)naphtho[2,3-*d*]oxaphosphole (4e)

3-Phosphino-2-naphthol (**3**, 0.480 g, 2.72 mmol) and 4-chloro-*N*-phenylbenzimidoyl chloride (2.22 g, 8.87 mmol) were added in a 250 mL round bottom flask with a stir bar and the flask was outfitted with a reflux condenser and flushed with nitrogen. THF (25 mL) was added by cannula and the solution was refluxed for 20 hours. The reaction mixture was taken into a dry box and filtered using glass fritted filter funnel. The solid was extracted 2 times with THF (~5 mL) and the combined filtrate was evaporated under vacuum yield a brown solid. The solid was dissolved in CH₂Cl₂ (~75 mL), washed successively with degassed solutions of aqueous HCl (1.2 M, 100 mL), aqueous NaOH (1 M, 100 mL) and distilled H₂O (100 mL). The solvent was removed under vacuum to yield a yellow solid which was washed with degassed ethanol (~150 mL) and then recrystallized from toluene at –45 °C to yield yellow solid **4e** (0.350 g, 43.2%). ¹H NMR: δ 8.51 (d, 1H, ³*J*_{PH} = 4.8 Hz), 8.15 (s, 1H), 8.03 (m, 2H), 7.95 (m, 2H), 7.50 (m, 2H), 7.43 (m, 2H); ³¹P{¹H} NMR: δ 85.8(s); ¹³C{¹H} NMR: δ 198.3 (d, *J*_{PC} = 54.7 Hz), 158.0 (d, *J*_{PC} = 3.8 Hz), 136.4 (d, *J*_{PC} = 37.0 Hz), 136.0 (d, *J*_{PC} = 6.0 Hz), 133.1 (d, *J*_{PC} = 13.1 Hz), 133.0 (d, *J*_{PC} = 2.6 Hz), 130.1 (d, *J*_{PC} = 10.6 Hz), 129.1, 129.0 (d, *J*_{PC} = 19.0 Hz), 127.8, 127.8, 126.3, 126.3 (d, *J*_{PC} = 14.9 Hz), 124.8, 109.1; UV (CH₂Cl₂): λ_{max}, nm (ε, M⁻¹ cm⁻¹) 357 (28 710); Fluorescence (CH₂Cl₂, 5 × 10⁻⁶ M): λ_{ex}, nm (Int.) 465 (661); Quantum Yield (CH₂Cl₂): Φ_F 0.128; mp 190–194 °C; Elemental analysis: Calc. for C₁₇H₁₀ClOP (M. W. 296.69), C 68.82%, H 3.40%; found: C 69.01%, H 3.32%.

2-(4-Bromophenyl)naphtho[2,3-*d*]oxaphosphole (4f)

3-Phosphino-2-naphthol (**3**, 0.600 g, 3.41 mmol) and 4-bromo-*N*-phenylbenzimidoyl chloride (**3**, 1.86 g, 6.31 mmol) were added in a 250 mL round bottom flask with a stir bar. The flask was outfitted with a reflux condenser and flushed with nitrogen. THF (30 mL) was added by cannula and the solution was refluxed for 20 hours. The reaction mixture was taken into a dry box and filtered using glass fritted filter funnel. The solid was extracted 2 times with THF (~5 mL), the combined filtration was evaporated under vacuum yield a brown solid. The solid was dissolved in CH₂Cl₂ (~75 mL), washed successively with degassed solutions of aqueous HCl (1.2 M, 100 mL), aqueous NaOH (1 M, 100 mL) and distilled H₂O (100 mL). The solvent was removed under vacuum to a yield yellow solid, which was washed with degassed ethanol (~150 mL) and recrystallized from toluene at -45 °C to yield yellow solid **4f** (0.380 g, 32.8%). ¹H NMR: δ 8.52 (d, 1H, ³J_{PH} = 4.8 Hz), 8.16 (s, 1H), 7.97 (m, 4H), 7.59 (d, 2H, ³J_{HH} = 8.4 Hz), 7.50 (m, 2H); ³¹P{¹H} NMR: δ 86.7 (s, 1P); ¹³C{¹H} NMR: δ 198.3 (d, J_{PC} = 54.8 Hz), 158.0 (d, J_{PC} = 3.6 Hz), 136.4 (d, J_{PC} = 37.0 Hz), 133.5 (d, J_{PC} = 13.1 Hz), 133.0 (d, J_{PC} = 2.7 Hz), 132.1, 130.2 (d, J_{PC} = 10.3 Hz), 129.0 (d, J_{PC} = 19.2 Hz), 127.8, 127.8, 126.5 (d, J_{PC} = 14.9 Hz), 126.3, 124.9, 124.3 (d, J_{PC} = 6.0 Hz), 109.2; UV (CH₂Cl₂): λ_{max}, nm (ε, M⁻¹ cm⁻¹) 357 (28086); Fluorescence (CH₂Cl₂, 5 × 10⁻⁶ M): λ_{ex}, nm (Int.) 464 (633); Quantum yield (CH₂Cl₂): Φ_F 0.125; mp 202–205 °C; HRMS *m/z*: 339.9655 (calc. 339.9653).

2-(4-Methoxyphenyl)naphtho[2,3-*d*]oxaphosphole (4g)

3-Phosphino-2-naphthol (**3**, 0.500 g, 2.84 mmol) and 4-methoxy-*N*-phenylbenzimidoyl chloride (1.68 g, 6.84 mmol) were added in a 250 mL round bottom flask with a stir bar. The flask was outfitted with a reflux condenser and flushed with nitrogen. THF (25 mL) was added by cannula and the solution was refluxed for 20 hours. The reaction mixture was taken into a dry box and filtered using glass fritted filter funnel. The solid was extracted 2 times with THF (~5 mL) and the combined filtrate was evaporated under vacuum yield a brown solid. The solid was dissolved in CH₂Cl₂ (~75 mL), washed successively with degassed solutions of aqueous HCl (1.2 M, 100 mL), aqueous NaOH (1 M, 100 mL) and distilled H₂O (100 mL). The solvent was removed under vacuum to yield a yellow solid which was washed with degassed ethanol (~150 mL) and recrystallized from toluene at -45 °C to yield yellow solid **4g** (0.600 g, 72.3%). ¹H NMR: δ 8.47 (d, 1H, ³J_{PH} = 4.8 Hz), 8.13 (s, 1H), 8.05 (m, 2H), 7.94 (m, 2H), 7.48 (m, 2H), 6.98 (m, 2H); ³¹P{¹H} NMR: δ 74.9 (s, 1P); ¹³C{¹H} NMR: δ 200.2 (d, J_{PC} = 56.2 Hz), 161.4 (d, J_{PC} = 4.8 Hz), 157.9 (d, J_{PC} = 3.2 Hz), 142.0 (d, J_{PC} = 20.1 Hz), 136.9 (d, J_{PC} = 37.3 Hz), 132.7 (d, J_{PC} = 2.4 Hz), 130.1 (d, J_{PC} = 9.8 Hz), 128.4 (d, J_{PC} = 19.3 Hz), 127.7, 127.7, 126.9 (d, J_{PC} = 14.5 Hz), 125.9, 124.6, 114.3, 108.8, 55.5; UV (CH₂Cl₂): λ_{max}, nm (ε, M⁻¹ cm⁻¹) 360 (23566); Fluorescence (CH₂Cl₂, 5 × 10⁻⁶ M): λ_{ex}, nm (Int.) 470 (876); Quantum yield (CH₂Cl₂): Φ_F 0.219; mp 195–198 °C; Elemental analysis: Calc. for C₁₈H₁₃O₂P (M. W. 292.27), C 73.91%, H 4.48%; found: C 73.40%, H 4.16%.

Acknowledgements

We thank the National Science Foundation for support (CHE-0748982 and CHE-1150721).

Notes and references

- J. Heinicke and A. Tzschach, *Z. Chemie*, 1980, **20**, 342–343.
- J. Heinicke and A. Tzschach, *Phosphorus, Sulfur Silicon Relat. Elem.*, 1985, **25**, 345–356.
- L. Nyulaszi, G. Csonka, J. Reffy, T. Veszpremi and J. Heinicke, *J. Organomet. Chem.*, 1989, **373**, 49–55.
- F. Mathey, *Phosphorus-Carbon Heterocyclic Chemistry: The Rise of a New Domain*, Pergamon, Amsterdam, 2001.
- K. B. Dillon, F. Mathey and J. F. Nixon, *Phosphorus: The Carbon Copy*, John Wiley & Sons, New York, 1998.
- V. R. Appel, F. Knoll and I. Ruppert, *Angew. Chem.*, 1981, **93**, 771–784.
- L. N. Markovski and V. D. Romanenko, *Tetrahedron*, 1989, **45**, 6019–6090.
- F. Mathey, *Acc. Chem. Res.*, 1992, **25**, 90–96.
- F. Mathey, *Angew. Chem., Int. Ed. Engl.*, 2003, **42**, 1578–1604.
- M. P. Washington, V. B. Gudimetla, F. L. Laughlin, N. Deligonul, S. He, J. L. Payton, M. C. Simpson and J. D. Protasiewicz, *J. Am. Chem. Soc.*, 2010, **132**, 4566–4567.
- (a) L. J. Higham, *The Primary Phosphine Renaissance in Phosphorus Compounds: Advanced Tools in Catalysis and Material Sciences*, ed. M. Peruzzini and L. Gonsalvi, Springer, Germany, 2011; (b) R. M. Hiney, A. Ficks, H. Müller-Bunz, D. G. Gilheany and L. J. Higham, *Air-stable Chiral Primary Phosphines: Part (i) Synthesis, Stability and Reactivity in Specialist Periodical Reports: Organometallic Chemistry*, ed. I. J. S. Fairlamb and J. M. Lynam, Royal Society of Chemistry, London, UK, 2011, pp. 27–45.
- Some reviews: (a) D. Lehnher and R. R. Tykwinski, *Materials*, 2010, **3**, 2772–2800; (b) Y. Kunugi, *J. Soc. Inorg. Mater., Jpn.*, 2010, **17**, 182–187; (c) Y. Yamashita, *Sci. Technol. Adv. Mater.*, 2009, **10**, No pp given (d) W. J. Potscavage Jr., A. Sharma and B. Kippelen, *Acc. Chem. Res.*, 2009, **42**, 1758–1767; (e) B. Nickel, *Organ. Electron.*, 2009, 301–315; (f) X. Feng, W. Pisula and K. Muellen, *Pure Appl. Chem.*, 2009, **81**, 2203–2224; (g) B. Nickel, M. Fiebig, S. Schiefer, M. Goellner, M. Huth, C. Erlen and P. Lugli, *Phys. Status Solidi A*, 2008, **205**, 526–533; (h) M. Kitamura and Y. Arakawa, *J. Phys.: Condens. Matter*, 2008, **20**, 184011–184016; (i) J. E. Anthony, *Angew. Chem., Int. Ed. Engl.*, 2008, **47**, 452–483; (j) M. T. Lloyd, J. E. Anthony and G. G. Malliaras, *Materials Today*, 2007, **10**, 34–41 edn.
- U. H. F. Bunz, *Pure Appl. Chem.*, 2010, **82**, 953–968.
- M. Hissler, P. W. Dyer and R. Reau, *Top. Curr. Chem.*, 2005, **250**, 127–163.
- Recent reports: (a) J.-H. Wan, W.-F. Fang, Y.-B. Li, X.-Q. Xiao, L.-H. Zhang, Z. Xu, J.-J. Peng and G.-Q. Lai, *Org. Biomol. Chem.*, 2012, **10**, 1459–1466; (b) Y. Ren and T. Baumgartner, *J. Am. Chem. Soc.*, 2011, **133**, 1328–1340; (c) Y. Matano, A. Saito, T. Fukushima, Y. Tokudome, F. Suzuki, D. Sakamaki, H. Kaji, A. Ito, K. Tanaka and H. Imahori, *Angew. Chem., Int. Ed.*, 2011, **50**, 8016–8020, S8016/8011–S8016/8027 (d) Y. Matano, Y. Kon, A. Saito, Y. Kimura, T. Murafuji and H. Imahori, *Chem. Lett.*, 2011, **40**, 919–921; (e) R. A. Krueger, T. J. Gordon, T. C. Sutherland and T. Baumgartner, *J. Polym. Sci., Part A Polym. Chem.*, 2011, **49**, 1201–1209; (f) S. Durben and T. Baumgartner, *Angew. Chem., Int. Ed.*, 2011, **50**, 6823–6836; (g) S. Durben and T. Baumgartner, *Angew. Chem., Int. Ed.*, 2011, **50**, 7948–7952; (h) T. Linder, T. C. Sutherland and T. Baumgartner, *Chem.–Eur. J.*, 2010, **16**, 7101–7105; (i) S. Durben, T. Linder and T. Baumgartner, *New J. Chem.*, 2010, **34**, 1585–1592; (j) D. R. Bai, C. Romero-Nieto and T. Baumgartner, *Dalton Trans.*, 2010, **39**, 1250–1260; (k) A. Saito, T. Miyajima, M. Nakashima, T. Fukushima, H. Kaji, Y. Matano and H. Imahori, *Chem.–Eur. J.*, 2009, **15**, 10000–10004; (l) Y. Dienes, M. Eggenstein, T. Karpati, T. C. Sutherland, L. Nyulaszi and T. Baumgartner, *Chem.–Eur. J.*, 2008, **14**, 9878–9889; (m) Y. Dienes, M. Eggenstein, T. Neumann, U. Englert and T. Baumgartner, *Dalton Trans.*, 2006, 1424–1433.
- B. Dhawan and D. Redmore, *J. Org. Chem.*, 1991, **56**, 833–835.
- B. Stewart, A. Harriman and L. J. Higham, *Organometallics*, 2011, **30**, 5338–5343.
- L. J. Higham, *Catal. Met. Complexes*, 2011, **37**, 1–19.
- M. M. Rauhut and H. A. Currier, *J. Org. Chem.*, 1961, **26**, 4626–4628.